

# Formation of environmentally friendly protective Ce<sub>2</sub>O<sub>3</sub>-CeO<sub>2</sub> conversion coatings on Al, modified by phosphate layers: chemical and electrochemical characterization

R. Andreeva<sup>1</sup>, A. Tsanev<sup>2</sup>, D. Stoychev<sup>1\*</sup>

<sup>1</sup>*Institute of Physical Chemistry "Acad. R. Kaishev" – BAS, Acad. G. Bonchev Str. Bl. 11, Sofia 1113, Bulgaria*

<sup>2</sup>*Institute of General and Inorganic Chemistry – BAS, Acad. G. Bonchev Str. Bl. 11, Sofia 1113, Bulgaria*

Received: May 10, 2022; Accepted: November 21, 2023

Conversion ceria coatings were deposited on substrates of Al-1050 in a solution containing CeCl<sub>3</sub>·7H<sub>2</sub>O and CuCl<sub>2</sub>·2H<sub>2</sub>O. The post-treatment of as deposited coatings was realized in phosphate-containing solutions: 0.08 M Na<sub>3</sub>PO<sub>4</sub> or 0.22 M NH<sub>4</sub>H<sub>2</sub>PO<sub>4</sub>. The XPS characterization of the surface of samples was carried out on an AXIS Supra electron spectrometer (Kratos-Analytical Ltd.). The electrochemical investigations and determination of the basic corrosion parameters ( $E_{\text{cor}}$ ,  $i_{\text{cor}}$ ,  $E_{\text{pit}}$ ,  $E_{\text{OCP}}$ ,  $R_p$ , CR, etc.) for the studied systems were carried out on a Gamry Interface 1000 (EISFR Analyzer EIS300). Based on the XPS investigations, it was ascertained that there is a substantial influence of the "pre-treatment" and "post-treatment" operations on the chemical composition and chemical state of the elements on the samples' surface. It is expressed by a strong decrease in the concentration of Al<sub>2</sub>O<sub>3</sub> and Ce<sub>2</sub>O<sub>3</sub>+CeO<sub>2</sub> components in the ceria coatings at the expense of formation of AlPO<sub>4</sub> and AlOOH, CePO<sub>4</sub>, as well as PO<sub>3</sub><sup>-</sup>, P<sub>2</sub>O<sub>5</sub> and P<sub>4</sub>O<sub>10</sub> compounds with Al and Ce.

The comparison of the results of  $R_p$  values and concentrations of Ce<sup>3+</sup>/Ce<sup>4+</sup>, Al and P shows that the changes in  $R_p$  and quantity of Ce<sup>4+</sup> and P on the surface of the studied samples are directly related. The supposed and proved formation of low-soluble corrosion products on the surface of the studied systems and accomplished synergic effect of protective action by the formed cerium and aluminum oxides/phosphates layers determine the increase of the  $R_p$  and decrease of  $i_{\text{cor}}$  and CR, respectively. It was also concluded that the mixed conversion layers are a more effective barrier for the chloride ions diffusion to the metal surface and increase the corrosion resistance of Al 1050 to pitting and general corrosion.

**Keywords:** aluminium, corrosion, ceria/phosphate conversion coatings

## INTRODUCTION

The attention in the application of ceria conversion coatings deposition on Al and its alloys is driven by the potential opportunity to replace highly toxic and carcinogenic Cr<sup>6+</sup>-containing conversion coatings [1]. The latter, though providing excellent corrosion protection for Al surfaces [2], need to be replaced with ecological alternatives, according to EU directives [3, 4]. Conversion layers based on lanthanide metals are considered among the most promising for this purpose [1, 5-12].

We have previously reported our findings regarding the effects of pre-treatment operations of Al substrates, covered with conversion ceria coatings (CCOC) and additionally post-treated in different types of phosphate-containing solutions (leading to the formation of thin phosphate layers (PhL(s)) on the surface chemical composition of the so formed Al/CCOC/PhL(s) systems. Based on the XPS investigations, a strong decrease in the concentration of Al<sub>2</sub>O<sub>3</sub> and Ce<sub>2</sub>O<sub>3</sub>+CeO<sub>2</sub> components in CCOC at the expense of the formation of AlPO<sub>4</sub> and AlOOH, CePO<sub>4</sub> as well as PO<sub>3</sub><sup>-</sup>, P<sub>2</sub>O<sub>5</sub> and P<sub>4</sub>O<sub>10</sub> compounds of Al and Ce [13] was established.

Having in mind these changes in the qualitative and quantitative composition on the surface of the studied systems, the aim of the present study was to obtain, include and comment additional corroborative in detail information about the influence of both "pre-treatment" and "post-treatment" operations connected to formation of CCOC and PhL(s) with improved corrosion-protective ability of Al 1050.

## EXPERIMENTAL

Layers of cerium oxide(s) (obtained by chemical immersion treatment) were deposited on substrates of "technically pure" Al 1050 (containing 0.40% Fe, 0.25% Si, 0.05% Mn, 0.05% Cu, 0.07% Zn, 0.05% Mg) selected as a model object by us as it finds wide range of applications as a construction material.

The studied samples of dimensions 2.5×2.5×0.1 cm, were cut out of rolled Al 1050 sheets. Their pre-treatment, as described in [14], involved degreasing in organic solvent and etching in 1.5 M NaOH (the abbreviator of these samples in the further text is "Al<sub>(NaOH)</sub>") or etching in 1.5 M NaOH and consecutive activation in 5 M HNO<sub>3</sub> (acidic deoxidation) at room temperature (abbreviator

\* To whom all correspondence should be sent:  
E-mail: stoychev@ipc.bas.bg

" $Al_{(NaOH\&HNO_3)}$ "). After each one of these operations, the obligatory standard rinsing of the samples was made with distilled water.

The formation of CCOC was implemented in a solution containing 0.5 M  $CeCl_3 \times 7H_2O$  (Alfa Aesar) +  $1 \times 10^{-5}$  M  $CuCl_2 \times 2H_2O$  (Merck). No  $H_2O_2$ , or other type of oxidizing agent, was added. The chemical process was carried out at pH = 4.1, temperature of 25 °C and time interval of deposition till 120 min as described in [15-18]. The abbreviators of these samples covered with CCOC, depending of pretreatment operations, are: " $Al_{(NaOH)/CCOC_{(Ce+Cu)}}$ " or " $Al_{(NaOH\&HNO_3)/CCOC_{(Ce+Cu)}}$ ". The thickness of the deposited CCOCs was 110 nm for the  $Al_{(NaOH)/CCOC_{(Ce+Cu)}}$  system and 212 nm for the  $Al_{(NaOH\&HNO_3)/CCOC_{(Ce+Cu)}}$  system (measurements based on XPS in-depth profiles, which allow to track changes of the ratio between the elements Ce, Al and O in the depth of  $CCOC_{(Ce+Cu)}$  [18]). After formation of CCOC, the specimens were rinsed fully in distilled water, dried at room temperature and kept in a desiccator (if it is necessary) for subsequent investigation or phosphate conversion treatment.

The post-treatment of as deposited on Al substrate thin ceria coatings, aiming at an additional formation of phosphate layers (PhL(s)) on them, was implemented in two types of phosphate-containing solutions: 0.08 M  $Na_3PO_4$  or 0.22 M  $NH_4H_2PO_4$  (Alfa Aesar), applied and studied in details as described in [19-22]. The working solutions were used at pH = ~4.4, temperature of deposition 85°C and time of immersion 5 min. For these cases the abbreviators of the as prepared samples are: " $Al_{(NaOH)/CCOC_{(Ce+Cu)}/PhL_{(Na_3PO_4)}}$ " or " $Al_{(NaOH)/CCOC_{(Ce+Cu)}/PhL_{(NH_4H_2PO_4)}}$ " and " $Al_{(NaOH\&HNO_3)/CCOC_{(Ce+Cu)}/PhL_{(Na_3PO_4)}}$ " or " $Al_{(NaOH\&HNO_3)/CCOC_{(Ce+Cu)}/PhL_{(NH_4H_2PO_4)}}$ ", respectively.

The X-ray photoelectron spectroscopy (XPS) aimed the investigation of the chemical composition and chemical state of the elements on the surface of the studied samples was studied on AXIS Supra electron-spectrometer (Kratos Analytical Ltd.) using monochromatic  $AlK\alpha$  radiation, with a photon energy of 1486.6 eV. The analysed area was 0.75 mm<sup>2</sup> as described in [13]. The chemical composition (in at. %) and state of elements of cerium-based CCOC on Al 1050, with different contents of  $Ce^{3+}$  ( $Ce_2O_3$ ) and  $Ce^{4+}$  ( $CeO_2$ ), was examined and determined for the as deposited samples before and after their phosphate post-treatment in solutions of  $Na_3PO_4$  or  $NH_4H_2PO_4$ , as well as after long exposure (up to 168/336 h) in model corrosion media.

The corrosion behavior of the samples was studied in a standard three-electrode cell (equipped with a reference calomel electrode) in 0.1 M NaCl ("p.a." Merck) model (open to air) corrosion medium (CM) at 25°C, frequently used for corrosion tests of Al protected by ceria conversion coatings. The anodic and cathodic polarization curves were obtained by means of a potentiostat/galvanostat Gamry Interface 1000, as described in [18]. Open circuit potential (OCP) transients and corrosion current ( $i_{corr}$  at  $E_{pit}$  for Al 1050 = -0.500 V) transients vs. time were plotted in the same CM. The investigations of the time-depending changes of polarization resistance ( $R_p$ ,  $\Omega m.cm^2$ ), as well as corrosion rate (CR,  $\mu m/year$ ) of studied samples (as deposited and after definite time of exposure (up to 168/336 h) in CM) were carried out on Gamry Interface 1000 (Software and Frequency Response Analyzer EIS300). All potentials were referenced to Ag/AgCl reference electrode (SCE). The scan range was  $\pm 15$  mV relative to corrosion potential ( $E_{cor}$ ) and the scanning was carried out in the anodic direction. The initial delay was 15 minutes, and the temperature was 25 C  $\pm$  0.5°C. The specimen's area exposed to corrosion in CM was 1.54 cm<sup>2</sup>. The reproducibility of all tests was an average of 3 samples per sample type.

## RESULTS AND DISCUSSION

### XPS investigations

The results from the XPS studies of the chemical composition and chemical state of the elements for the studied systems are represented in Figs. 1 - 3 and in Tables 1, 2. The comparison of the compositions of samples, whose substrates have been pretreated in NaOH, with those, whose substrates have been pretreated in both NaOH and  $HNO_3$ , shows that in case of pretreatment only with NaOH, the concentration of Al (Al oxide/hydroxide, respectively) on the surface is high (Table 1). In the case of as-deposited CCOC (Table 1, samples a and d, obtained in  $Ce^{3+}$  and  $Cu^{2+}$  containing conversion solution) it is 21.2 % and 6.3 %, respectively; for the couple of samples, covered with CCOC and post-treated in  $Na_3PO_4$  (Table 1, samples b and e) it is 10.7 and 0.5 %, respectively while for the samples covered with CCOC and post-treated in  $NH_4H_2PO_4$  (Table 1, samples c and f) it is 7.6 and 4.8 %, respectively. The Ce concentration ( $Ce_2O_3$  and  $CeO_2$ , respectively) change for the same samples is inverted. This change is also inverted for the concentration of P on the COCC deposited phosphate layers (Table 1 (b and e), and (c and f)). These „inverted“ relationships are connected to forming cathode areas of electroless-deposited

copper on the Al surface. They are deposited preferentially on the aggregates of Al<sub>3</sub>Fe intermetallic phase of Al 1050 [14], which gain eminence after additional treatment in HNO<sub>3</sub> (Table 1 (e and f)). It is important to note the considerable result presented in Table 1 about the concentration

change of Ce<sup>4+</sup> (CeO<sub>2</sub>) depending on the pretreatment of the Al support. This unambiguously shows that copper deposited on the Al surfaces catalyses forming of CCOC (Table 1) [17, 18]. Below, these results and conclusions are exposed and commented in detail.

**Table 1.** Chemical composition and chemical state of the elements on the surface of the studied samples.

Sample	O	Al	Ce <sub>total</sub> , (Ce <sup>3+</sup> +Ce <sup>4+</sup> )	Cu	P	Ce <sup>4+</sup> , % of Ce <sub>total</sub>
a-Al <sub>(NaOH)</sub> /CCOC <sub>(Ce+Cu)</sub>	71.9	21.2	6.9	0	-	79
b-Al <sub>(NaOH)</sub> /CCOC <sub>(Ce+Cu)</sub> /PhL <sub>Na<sub>3</sub>PO<sub>4</sub></sub>	73.7	10.7	2.8	0	12.9	23
c-Al <sub>(NaOH)</sub> /CCOC <sub>(Ce+Cu)</sub> /PhL <sub>NH<sub>4</sub>H<sub>2</sub>PO<sub>4</sub></sub>	76.3	7.6	1.4	0.7	14.1	11
d-Al <sub>(NaOH&amp;HNO<sub>3</sub>)</sub> /CCOC <sub>(Ce+Cu)</sub>	75.7	5.9	17.2	1.2	-	85
e-Al <sub>(NaOH&amp;HNO<sub>3</sub>)</sub> /CCOC <sub>(Ce+Cu)</sub> /PhL <sub>Na<sub>3</sub>PO<sub>4</sub></sub>	70.1	0.5	10.0	2.6	16.8	0
f-Al <sub>(NaOH&amp;HNO<sub>3</sub>)</sub> /CCOC <sub>(Ce+Cu)</sub> /PhL <sub>NH<sub>4</sub>H<sub>2</sub>PO<sub>4</sub></sub>	75.3	4.8	4.5	0.8	14.7	35

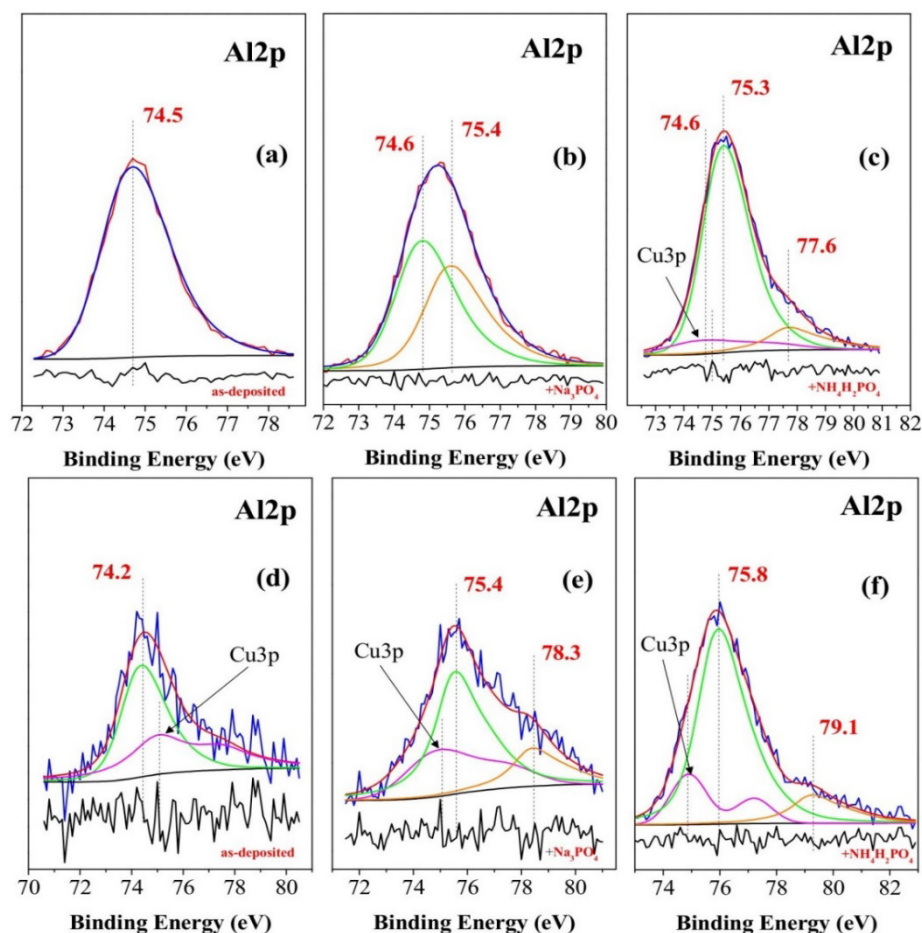


**Fig. 1.** XPS Al<sub>2</sub>p spectra obtained for as-deposited CCOC (a, d) and after its post-treatment in Na<sub>3</sub>PO<sub>4</sub> (b, e) or NH<sub>4</sub>H<sub>2</sub>PO<sub>4</sub> (c, f). The peak contributions are colored in green and orange whereas their sum is marked in red. The difference between experimental and deconvoluted spectra is indicated in the inset below. Violet peak(s) on Figs. 1(c – f) show the presence of copper (Cu<sub>3</sub>p) which is a component of CCOC.

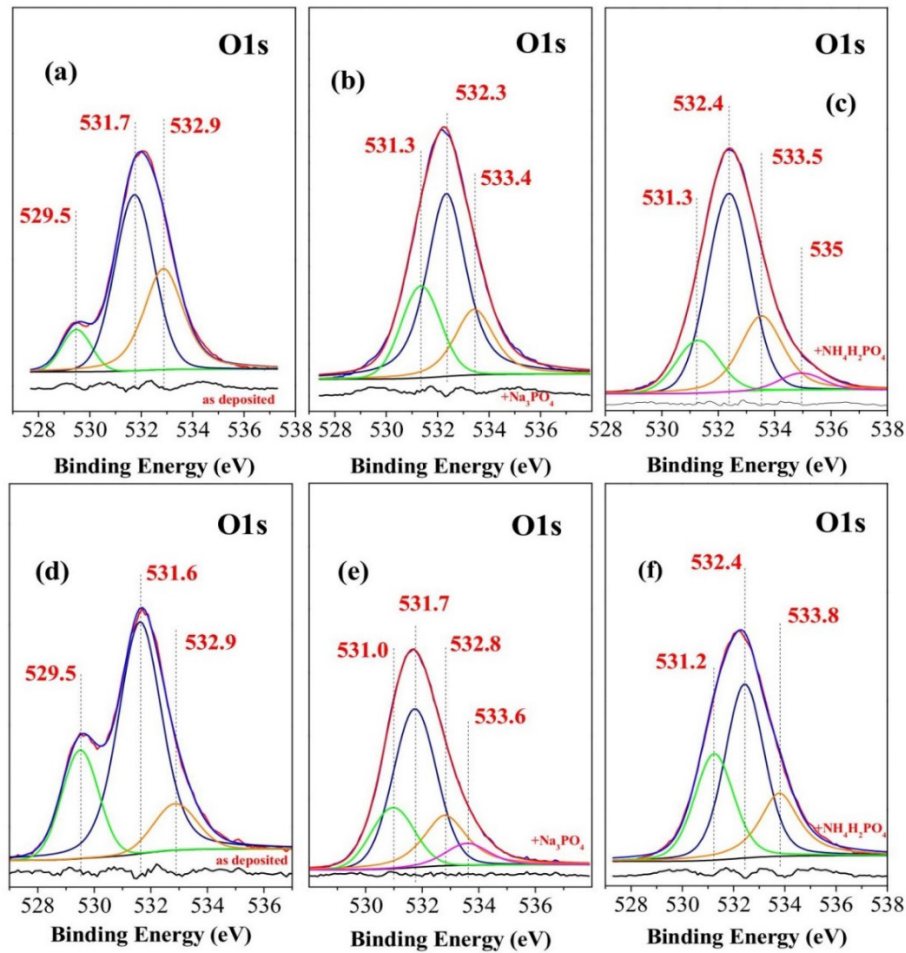


**Fig. 2.** XPS O1s spectra obtained for as-deposited CCOC (a, d) and after its post-treatment in  $Na_3PO_4$  (b, e) or  $NH_4H_2PO_4$  (c, f). The peak contributions are colored in green, orange and pink whereas their sum is marked in red. The difference between experimental and deconvoluted spectra is indicated in the inset below.

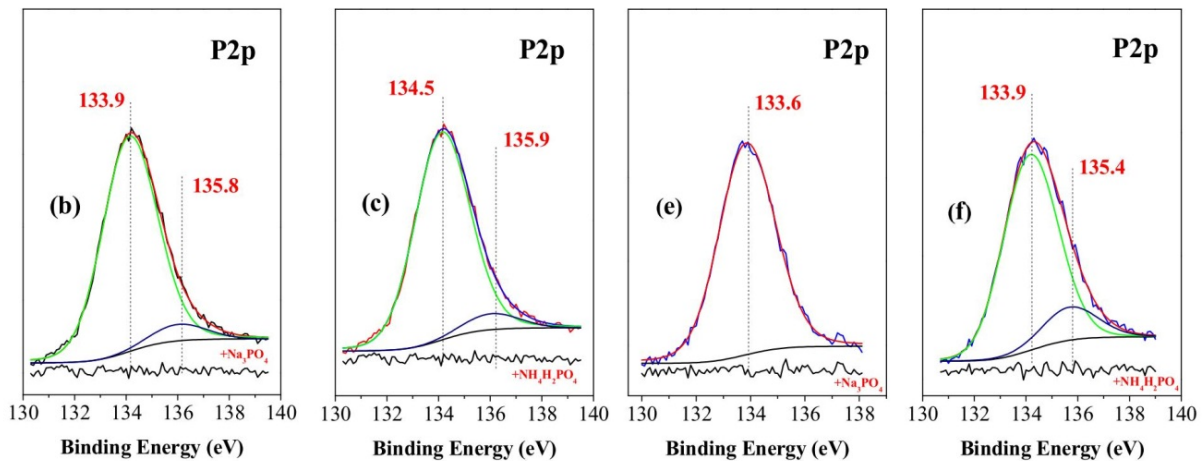


**Fig. 3.** XPS P2p spectra obtained for CCOC after its post-treatment in  $Na_3PO_4$  (b, e) or  $NH_4H_2PO_4$  (c, f). The peak contributions are colored in green and blue whereas their sum is marked in red. The difference between experimental and deconvoluted spectra is indicated in the inset below.

Fig. 1 presents the deconvoluted peaks of the characteristic Al2p-spectra for the studied samples.

In the case of as-deposited  $CCOC_{(Ce+Cu)}$  (Fig. 1a) a single peak was registered at 74.2 – 74.5 eV,

revealing the presence of Al on the surface only in the form of  $Al_2O_3$ . The deconvolution of O1s – (Fig. 2d) confirms this fact. The spectra of O1s consist of three peaks. The one with the lowest energy at 529.5 eV corresponds to oxygen species bonded in the crystal lattice of the  $CeO_2$  [24]. The peaks, positioned at 531.6-531.7 eV, correspond to oxygen bound in  $Al_2O_3$  [24]. In the case of sample a- $Al_{(NaOH)}/CCOC_{(Ce+Cu)}$ , the ratio between the areas of the Al2p-peak and the respective O1s-peak actually corresponds to the stoichiometric ratio 2:3. In the case of sample d- $Al_{(NaOH+HNO_3)}/CCOC_{(Ce+Cu)}$  a large excess of oxygen is registered, which could be due to the effect of screening by oxygen atoms (in the system only Al and Ce are present, while the area for just this O1s-peak is much larger than the stoichiometric quantity, calculated on the basis of the areas of Ce3d and Al2p peaks).

It is important to note that the registered Ce3d-spectra are characterized by a complex structure due to strong final photoelectron effects involving the influence of the oxygen ligands from chemical bonds with Ce [25]. According to [25] we can calculate the relative concentrations of  $Ce^{4+}$  and  $Ce^{3+}$  ions with respect to the total amount of Ce. These results are shown in Table 1. The highest relative concentrations of  $Ce^{4+}$  ions as 79% and 85% are observed in the samples a- $Al_{(NaOH)}/CCOC_{(Ce+Cu)}$  and d- $Al_{(NaOH+HNO_3)}/CCOC_{(Ce+Cu)}$ , respectively. This is a very useful and important information, in view of the established influence of  $Ce^{4+}$  and  $Ce^{3+}$  (having in mind the lower solubility of  $CeO_2$  in comparison with the soluble  $Ce_2O_3$ ) on the corrosion-protection ability of CCOC [18].

The spectra of Al2p of samples, treated with  $Na_3PO_4$ , are presented in Fig. 1 (b and e). In the case of sample b- $Al_{(NaOH)}/CCOC_{(Ce+Cu)}/PhL_{Na_3PO_4}$  (pretreated in NaOH) - Fig. 1b - two peaks appear in the spectrum of Al2p at 74.6 and 75.4 eV. The peak, located at 74.6 eV, can be associated with a mixture of  $Al_2O_3$  and non-stoichiometric Al-hydroxide. The other peak, positioned at 75.4 eV can be attributed to the presence of  $AlPO_4$  [26]. The quantitative ratio between the two phases is approximately 1:1. In contrast to it, the spectrum of Al2p for the sample e- $Al_{(NaOH+HNO_3)}/CCOC_{(Ce+Cu)}/PhL_{Na_3PO_4}$ , treated in advance in NaOH &  $HNO_3$  and post-treated in  $Na_3PO_4$  has the lowest intensity and noise due to the thick coating of the sample, covered with phosphate layer (Fig. 1e [23]). A deconvolution allows to see a peak at 75.4 eV, an indication about the presence mainly of  $AlPO_4$ , whereupon presence of nonstoichiometric  $AlOOH$  [27] is a possibility.

The deconvolution of the O1s peaks for both samples (Fig. 2 (b and e)) confirms the above-made

conclusions. The spectrum of O1s for both samples is deconvoluted into two basic peaks – a first one at 531.0 – 531.3 eV, corresponding to oxygen in the lattice of  $Ce^{3+}$ . The second one, located at 531.7 and at 532.3 eV corresponds to oxygen in the crystal lattice of metal phosphate. The other peaks at 532.8, 533.4 and 533.6 eV could be attributed to the presence, respectively, of hydroxyl groups, crystallized water and  $H_3O^+$ -groups. Their quantities were estimated based on the integral areas of their peaks [23].

The deconvolution of the P2p peaks (Fig. 3) shows that in both types of phosphate treatment metal phosphate phases are formed [28]. In both samples the phosphorus peak is positioned at 133.6 and 133.9 eV. In the case of the sample, pretreated only in NaOH, these phosphates cover the surface in a thicker way. In this sample a second phosphorus peak of lower intensity at 135.8 eV is also present, which could correspond to the presence of phosphorus compounds from the type of  $P_2O_5$  or  $P_4O_{10}$  [29].

The concentration of  $Ce^{4+}$  calculated from the spectrum of Ce3d (Table 1), shows that the phosphate treatment with  $Na_3PO_4$  decreases the concentration of  $Ce^{4+}$  in the conversion layer [29]. Thereupon, in the sample, pretreated in NaOH, the content of  $Ce^{4+}$  is 23% of the total amount of cerium oxide, while in the case of the sample, pretreated in NaOH& $HNO_3$   $Ce^{4+}$  is practically absent (Table 1).

For the samples, pretreated in NaOH or in NaOH &  $HNO_3$ , followed by post-treatment with  $NH_4H_2PO_4$ , the Al2p spectra are given in Fig. 1 (c and f). Here, in both samples one registers a single peak, located at 75.3 – 75.8 eV. This peak is characteristic for Al, bonded with phosphate groups (P-O-Me) [30]. The second peaks for both samples, respectively at 77.6 and at 79.1 eV, are due to the presence of particles with different sizes. Peaks, characteristic for oxides or hydroxides of aluminum are missing. At the same time the characteristic peaks of O1s for these two samples (Fig. 2 (c and f)), are splitted into three basic peaks. The peak at 531.3 eV can be associated with the presence of oxygen, bonded in the lattice of  $Al_2O_3$  and  $Ce_2O_3$  [29]. The second peak at 533.4 eV can be attributed again to the presence of oxygen, involved in P-O-Me – bonding [24]. The third peak, at approximately 533.5, 533.8 eV, is due to the presence of adsorbed or crystallized water.

The P2p-peak of the sample, pretreated in NaOH and post-treated in  $Na_3PO_4$ , consists of two components (Fig. 3b). The one, having the highest intensity at 133.9 eV, is due to the presence of  $PO_3^-$  - groups. The second one at 135.8 eV again can be

associated with the presence of phosphorus compounds of the type P<sub>2</sub>O<sub>5</sub> or P<sub>4</sub>O<sub>10</sub> [31]. The spectrum of the sample, pretreated in NaOH & HNO<sub>3</sub> and post-treated in Na<sub>3</sub>PO<sub>4</sub>, consists of one single P2p - peak at 133.6 eV (Fig. 3e), due to PO<sub>4</sub><sup>3-</sup> - groups. Comparing the peak areas for P2p, Al2p and Ce3d shows that the quantity of elemental phosphorus is much higher than needed for the

formation of stoichiometric phosphate compounds of aluminum and cerium [23].

The analysis of the XPS spectra of the systems under consideration allows to draw a conclusion about the composition of the most probable phases, formed on the aluminum surface. They are listed in Table 2.

**Table 2.** The most probable phases on the aluminum surface according to the analysis of the XPS spectra.

Sample	Al	Ce	P
a-Al <sub>(NaOH)</sub> /CCOC <sub>(Ce+Cu)</sub>	Al <sub>2</sub> O <sub>3</sub>	Ce <sub>2</sub> O <sub>3</sub> <sup>+</sup> CeO <sub>2</sub>	-
b-Al <sub>(NaOH)</sub> /CCOC <sub>(Ce+Cu)</sub> /PhL <sub>Na<sub>3</sub>PO<sub>4</sub></sub>	AlPO <sub>4</sub> , AlOOH	Ce <sub>2</sub> O <sub>3</sub> <sup>+</sup> CeO <sub>2</sub> CePO <sub>4</sub>	PO <sub>4</sub> <sup>3-</sup> P <sub>2</sub> O <sub>5</sub> (P <sub>4</sub> O <sub>10</sub> )
c-Al <sub>(NaOH)</sub> /CCOC <sub>(Ce+Cu)</sub> /PhL <sub>NH<sub>4</sub>H<sub>2</sub>PO<sub>4</sub></sub>	AlPO <sub>4</sub>	CePO <sub>4</sub>	PO <sub>3</sub> <sup>-</sup> P <sub>2</sub> O <sub>5</sub> (P <sub>4</sub> O <sub>10</sub> )
d-Al <sub>(NaOH&amp;HNO<sub>3</sub>)</sub> /CCOC <sub>(Ce+Cu)</sub>	Al <sub>2</sub> O <sub>3</sub>	Ce <sub>2</sub> O <sub>3</sub> <sup>+</sup> CeO <sub>2</sub>	-
e-Al <sub>(NaOH&amp;HNO<sub>3</sub>)</sub> /CCOC <sub>(Ce+Cu)</sub> /PhL <sub>Na<sub>3</sub>PO<sub>4</sub></sub>	AlOOH AlPO <sub>4</sub>	Ce <sub>2</sub> O <sub>3</sub> <sup>+</sup> CeO <sub>2</sub> CePO <sub>4</sub>	PO <sub>4</sub> <sup>3-</sup>
f-Al <sub>(NaOH&amp;HNO<sub>3</sub>)</sub> /CCOC <sub>(Ce+Cu)</sub> /PhL <sub>NH<sub>4</sub>H<sub>2</sub>PO<sub>4</sub></sub>	AlPO <sub>4</sub>	CePO <sub>4</sub>	PO <sub>4</sub> <sup>3-</sup> P <sub>2</sub> O <sub>5</sub> (P <sub>4</sub> O <sub>10</sub> )

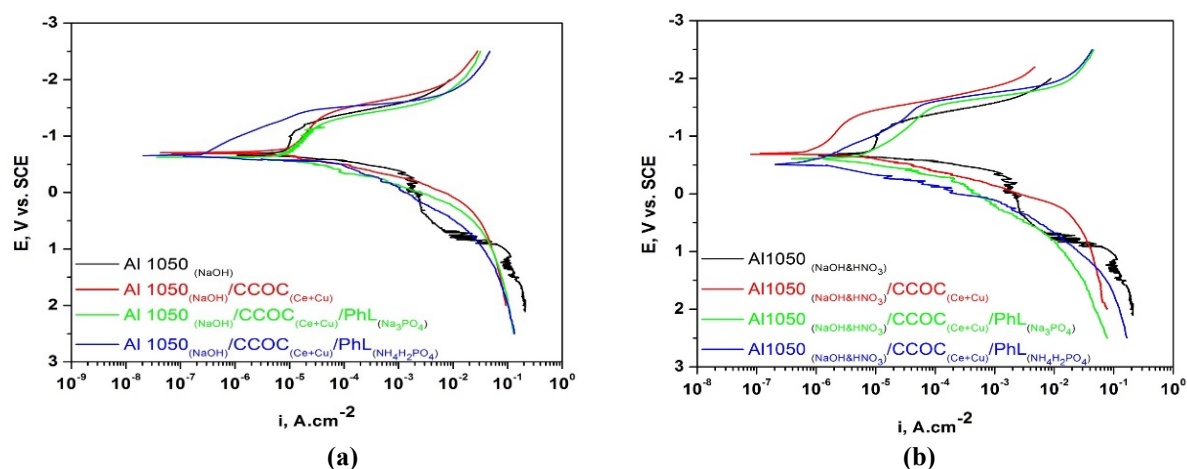


**Fig. 4.** Tafel polarization curves of the studied systems, Al substrate(s) of which are pretreated in 1.5 M NaOH (a) or in 1.5 M NaOH and 5 M HNO<sub>3</sub> (b).

**Table 3.** Electrochemical parameters of the studied systems determined from potentiodynamic polarization E-Ig i curves: i<sub>cor</sub> – corrosion current; E<sub>cor</sub> – corrosion potential; Z – degree of protection.

Sample	i <sub>cor</sub> , A.cm <sup>-2</sup>	E <sub>cor</sub> , V	Z, %
Al <sub>(NaOH)</sub>	8.0×10 <sup>-6</sup>	-0.660	
a-Al <sub>(NaOH)</sub> /CCOC <sub>(Ce+Cu)</sub>	1.0×10 <sup>-6</sup>	-0.695	87.5
b-Al <sub>(NaOH)</sub> /CCOC <sub>(Ce+Cu)</sub> /PhL <sub>(Na<sub>3</sub>PO<sub>4</sub>)</sub>	6.3×10 <sup>-6</sup>	-0.612	21.3
c-Al <sub>(NaOH)</sub> /CCOC <sub>(Ce+Cu)</sub> /PhL <sub>(NH<sub>4</sub>H<sub>2</sub>PO<sub>4</sub>)</sub>	2.4×10 <sup>-7</sup>	-0.649	97.0
d-Al <sub>(NaOH&amp;HNO<sub>3</sub>)</sub> /CCOC <sub>(Ce+Cu)</sub>	4.0×10 <sup>-7</sup>	-0.700	95.0
e-Al <sub>(NaOH&amp;HNO<sub>3</sub>)</sub> /CCOC <sub>(Ce+Cu)</sub> /PhL <sub>(Na<sub>3</sub>PO<sub>4</sub>)</sub>	3.5×10 <sup>-6</sup>	-0.586	56.3
f-Al <sub>(NaOH&amp;HNO<sub>3</sub>)</sub> /CCOC <sub>(Ce+Cu)</sub> /PhL <sub>(NH<sub>4</sub>H<sub>2</sub>PO<sub>4</sub>)</sub>	8.9×10 <sup>-7</sup>	-0.531	88.9

The results shown above give us the reason to draw the conclusion, that this way of pre-treatment for Al substrate and the application of additional post-treatment of the CCOC deposited on it in  $Na_3PO_4$  or  $NH_4H_2PO_4$  lead to the formation of PhL(s) on the surface of the CCOC. This conclusion has been reached also by some other authors. For instance, according to [27], in case of similar treatment, the surface of Al 2024-T3 was completely phosphated. It is logical to suppose that the additional PhL(s) being formed will exert synergistic effect, from corrosion-protection point of view, together with CCOC in regard to the Al substrate.

#### *Electrochemical and corrosion investigations of the studied systems*

*Polarization investigations.* Fig. 4 presents the polarization curves in coordinates E-Ig i, obtained in 0.1 M NaCl for samples having formed CCOC after preliminary activation of the Al substrate in a solution of NaOH (Fig. 4a) and two-stage preliminary treatment in solutions of NaOH and  $HNO_3$  (Fig. 4b), sealed in solutions of  $Na_3PO_4$  or  $NH_4H_2PO_4$ , respectively.

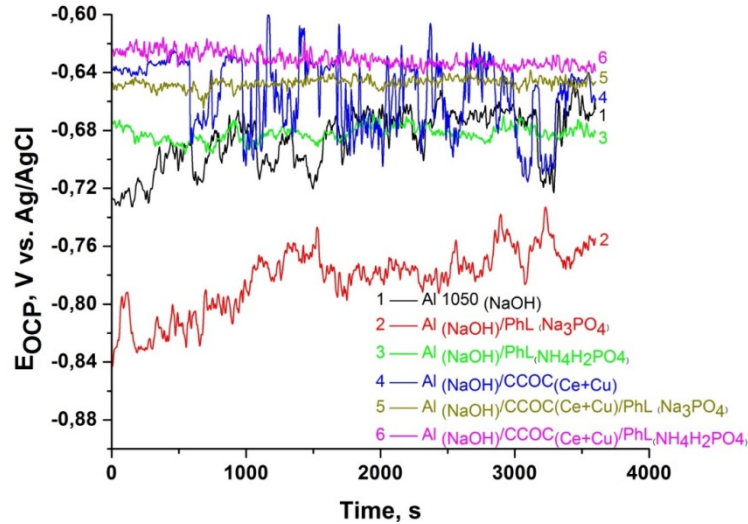
One can see in Fig. 4a that after the pre-treatment of the aluminum substrate in a solution of NaOH, the sealing of the samples in a solution of  $NH_4H_2PO_4$  (the system  $Al_{(NaOH)}/CCOC_{(Ce+Cu)}/PhL_{(NH_4H_2PO_4)}$ ) determines the strong influence on the kinetics of the cathode reaction of reduction of oxygen in the CM, which is reflected on the enhancement of the corrosion protection degree Z reaching 97 % (Table 3). When the preliminary activation of the aluminum substrate is carried out in a solution of NaOH and  $HNO_3$  (Fig. 4b), the post-treatment in both types of phosphate solutions leads to a substantial shift of the anodic potentiodynamic curves towards more positive potentials and lower values of the corrosion currents under the conditions of anodic polarization (Table 3). In this case, the treatment in a solution of  $NH_4H_2PO_4$  exerts a more strongly expressed barrier effect in regard to the processes of anodic dissolution of the aluminum substrate. A characteristic feature of the anodic potentiodynamic curves is the absence of a zone of passive state, which justifies the consideration that the corrosion potential of the studied systems coincides with the potential of

pitting formation. This coincidence is a prerequisite for the local character of the corrosion process under the conditions of stationary corrosion. This means that the definite protection degree Z (Table 3) obtained by treatment of the samples in a solution of  $NH_4H_2PO_4$  characterizes both the protection from total corrosion and from local corrosion. The results obtained show that the combination of phosphate and ceria conversion layers are not only static barrier coatings, but they also change the kinetics of the conjugated electrochemical reactions characterizing the corrosion process in  $Cl^-$  containing media, i.e. they determine the electrochemical protection of the Al substrate.

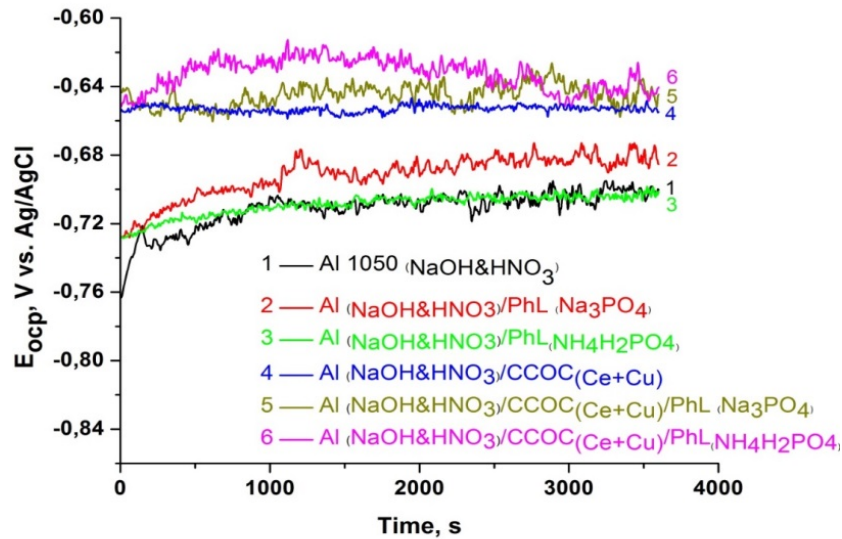
These results, obtained under conditions of external polarization (potentiodynamic polarization - PDP), inform on the kinetics of the related corrosion process reactions, but do not fully characterize them since the real corrosion processes occur at the open circuit potential ( $OCP/E_{OCP}$ ). At the same time, it is shown that the change in OCP as a function of immersion time can be used to monitor the chemical stability and corrosion process of the Al alloys [32]. Although OCP does not provide any direct information on the corrosion kinetics, it suggests the corrosion susceptibility [33]. To gain the needed additional insights, we conducted investigations of self-occurring corrosion processes in the systems of interest at OCP and at the potential of pitting corrosion ( $E_{pit}$ ), by following:

- the change in OCP values monitored through  $E_{OCP}$  vs. time plot;
- the changes in anodic current ( $i_a$ ) transients at  $E_{pit}$ ;
- the changes in  $R_p$  as a function of samples exposure time in CM (in OCP conditions) and the related change in CR.

*Open circuit potential measurements.* The bare  $Al_{(NaOH)}$  and the coupons of the systems  $Al_{(NaOH)}/PhL_{(Na_3PO_4)}$ ;  $Al_{(NaOH)}/PhL_{(NH_4H_2PO_4)}$ ;  $Al_{(NaOH)}/CCOC_{(Ce+Cu)}$ ;  $Al_{(NaOH)}/CCOC_{(Ce+Cu)}/PhL_{(Na_3PO_4)}$  and  $Al_{(NaOH)}/CCOC_{(Ce+Cu)}/PhL_{(NH_4H_2PO_4)}$  were immersed in CM for 1 hour. During this time of immersion, the changes in  $E_{OCP}$  vs. time for these samples were recorded and are given in Fig. 5a.



(a)



(b)

**Fig. 5.** OCP vs. time plots during immersion in 0.1M NaCl of the studied systems, Al substrate(s) are pretreated in 1.5 M NaOH (a) or in 1.5 M NaOH and 5 M  $HNO_3$  (b).

For the bare  $Al_{(NaOH)}$ , the registered average value for  $E_{OCP}$  is  $\sim -686$  mV with big fluctuations (black curve 1) indicating the dissimilarities in potential of different intermetallic inclusions, metastable pit formation and re-passivation in the CM. For the system  $Al_{(NaOH)}/PhL_{(Na_3PO_4)}$  (red curve 2), there was a large decrease in  $E_{OCP}$  (initially to  $\sim -820$  mV, and it started to stabilize after 1500-rd s to  $\sim -780$  mV) which could be due to the progress of heterogeneous reactions. These effects could be due to the saturation of the  $AlPO_4$  surface with  $Cl^-/H_2O$ . The fluctuation in  $E_{OCP}$  also could be due to the partial incorporation of the aqua ion and formation of Al oxides/hydroxides. When it was exposed to the

aggressive environment, the corrosive  $Cl^-$  ions penetrated through the active region and lead to more negative  $E_{OCP}$ .  $Al_{(NaOH)}/PhL_{(NH_4H_2PO_4)}$  coupon (the green curve 3) showed position and fluctuations in the  $E_{OCP}$  similar to that for the bare  $Al_{(NaOH)}$ .  $E_{OCP}$  fluctuations are most notable for the  $Al_{(NaOH)}/CCOC_{(Ce+Cu)}$  system (blue curve 4), with an average  $E_{OCP}$  value of  $\sim -665$  mV. However, when  $Al_{(NaOH)}/CCOC_{(Ce+Cu)}$  is sealed in a solution of  $Na_3PO_4$  (the  $Al_{(NaOH)}/CCOC_{(Ce+Cu)}/PhL_{(Na_3PO_4)}$  system – dark yellow curve 5) -  $E_{OCP}$  shifts further in a positive direction (to  $\sim -647$  mV). Post-treatment of  $Al_{(NaOH)}/CCOC_{(Ce+Cu)}$  in  $NH_4H_2PO_4$  (the  $Al_{(NaOH)}/CCOC_{(Ce+Cu)}/PhL_{(NH_4H_2PO_4)}$  system - magenta curve 6) brings an even greater shift in  $E_{OCP}$  (to  $\sim -630$

mV), which is of  $\sim 55$  mV more positive than that of bare  $Al_{(NaOH)}$ . This shift in  $E_{OCP}$  distinguishes the  $Al_{(NaOH)}/CCOC_{(Ce+Cu)}/PhL_{(NH_4H_2PO_4)}$  system as the most stable one from a corrosion-protection perspective. These conclusions are in good agreement with the noted effective increase in the protective effect of CCOC following the additional deposition of PhLs, including mixed  $AlPO_4$  and  $AlOOH$ ,  $CePO_4$  as well as  $PO_3^-$ ,  $P_2O_5$  and  $P_4O_{10}$  compounds with Al and Ce marked and discussed above.

It is seen on Fig. 5b that during the immersion, the course and changes in OCP for the bare  $Al_{(NaOH\&HNO_3)}$  sample (black transient 1) and the coupon of the system  $Al_{(NaOH\&HNO_3)}/PhL_{(NH_4H_2PO_4)}$  (green transient 3) practically coincide at about  $-0.705$  V. A small displacement in positive direction (to  $\sim -0.685$  V) is observed for the system  $Al_{(NaOH\&HNO_3)}/PhL_{(Na_3PO_4)}$  (red transient 2). The consecutive increase for the values of  $E_{OCP}$  have been observed for: the covered with CCOC Al substrate (the system  $Al_{(NaOH\&HNO_3)}/CCOC_{(Ce+Cu)}$  (blue transient 4)) – to  $\sim -0.655$  V and post-treated in  $Na_3PO_4$  or  $NH_4H_2PO_4$   $Al_{(NaOH\&HNO_3)}/CCOC_{(Ce+Cu)}$  system – the mixed systems  $Al_{(NaOH\&HNO_3)}/CCOC_{(Ce+Cu)}/PhL_{(NH_4H_2PO_4)}$  (dark yellow transient 5) – to  $\sim -0.645$  V and  $Al_{(NaOH\&HNO_3)}/CCOC_{(Ce+Cu)}/PhL_{(NH_4H_2PO_4)}$  (magenta transient 6) – to  $\sim -0.640$  V, respectively. The fluctuations registered practically for all studied systems indicate, (similar to that on Fig. 5a) dissimilarities in potential of different intermetallic inclusions, metastable pit formation and re-passivation in the CM. Also, the fluctuation in OCP could be due as well to the partial incorporation of the aqua ion and formation of Al oxides/hydroxides. When the samples have been exposed to the aggressive environment, the corrosive

ions penetrated through the active regions and lead to more negative OCP.

Totally, the average change of  $E_{OCP}$  in positive direction under the action of phosphate post-treatment of the CCOC is  $\sim 0.055$  V. This positive shift (in the area of  $E_{OCP}$  from  $\sim -0.705$  to  $\sim -0.640$  V vs. Ag/AgCl) compared to the bare  $Al_{(NaOH\&HNO_3)}$  indicated the effective incorporation and stabilization of the phosphate modified systems.

**Chronoamperometric investigations.** In these investigations, polarizing the samples anodically at  $E_{pit}$  ( $-0.500$  V vs. SCE), we aimed to approach to a maximal extent the actual corrosion process, respectively to characterize corrosion in view of pitting corrosion, which is a basic characteristic of aluminum and its alloys in  $Cl^-$ -containing CM [19, 34]. Based on the course of the registered curves we could judge the character of the corrosion attack and the appearance of pitting damages. Fig. 6 presents the results of the studied samples. On Fig. 6a we observe that for the Al substrate ( $Al_{(NaOH)}$ ) the corrosion current density is sharply increased (until reaching the  $\sim 180$ -th second of exposure), whereupon the surface film on the Al is disrupted (Fig. 6a, curve 1), which is a prerequisite for the appearance and development of pitting corrosion during the interaction with the CM. After breaking through the passive film, there starts a process of local corrosion characterized by values of the anodic current ( $i_a$ ) and current oscillations specific for it, owing to unstable pittings which are repassivated/activated. Similar behavior is also observed for the current transients of the  $Al_{(NaOH)}/PhL_{(Na_3PO_4)}$  and  $Al_{(NaOH)}/PhL_{(NH_4H_2PO_4)}$  systems (Fig. 6a, curves 2, 3).

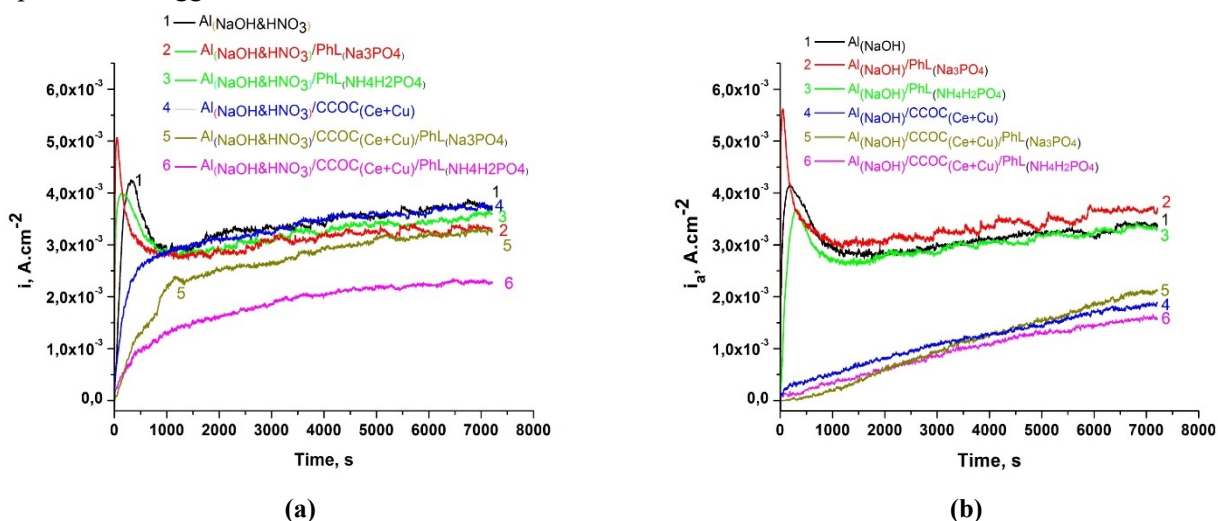


Fig. 6. Chronoamperometric transients of the studied systems, Al substrate(s) of which are pretreated in 1.5 M NaOH (a) or in 1.5 M NaOH and 5 M HNO<sub>3</sub> (b) in 0.1M NaCl at the  $E_{pit}$  of Al 1050.

The course of the current transients is conceptually different for samples protected with CCOC and post-treated in phosphate solutions (Fig. 6a, curves 4-6). At the same time there are no current fluctuations characteristic for localized breakdown of the passive film, which leads to the initiation and growth of corrosion pits in CM. The transients have a course characteristic of processes of general corrosion.  $i_a$  of the  $Al_{(NaOH)}/CCOC_{(Ce+Cu)}$  system increases gradually, remaining about three times lower ( $1.2 \times 10^{-3}$  A.cm<sup>-2</sup> vs.  $3.2 \times 10^{-3}$ ) than  $i_a$  of  $Al_{(NaOH)}$ . This difference in  $i_a$  drop is enhanced by ~ 10%, resp. 20%, for the  $Al_{(NaOH)}/CCOC_{(Ce+Cu)}/PhL_{(Na_3PO_4)}$  and  $Al_{(NaOH)}/CCOC_{(Ce+Cu)}/PhL_{(NH_4H_2PO_4)}$  systems (Fig. 6a, curves 5 and 6).

Fig. 6b presents the results of the chronoamperometric investigations using the samples, obtained after preliminary treatment of the Al substrate consecutively in NaOH&HNO<sub>3</sub>. We observed that for  $Al_{(NaOH\&HNO_3)}$ , after its immersion in the CM at  $E_{pit}$ , the corrosion current density is sharply increased (until reaching the ~380-th second of exposure) up to values of ~  $4.22 \times 10^{-3}$  A.cm<sup>-2</sup>, whereupon the surface film on the aluminum is disrupted (Fig. 6b, black curve 1), which is a prerequisite for the appearance and development of pitting corrosion during the interaction with the CM. After breaking through the passive film, there starts a process of local corrosion characterized by values of the anodic current ( $i_a$ ) of ~  $3.40 \times 10^{-3}$  A.cm<sup>-2</sup> (at 3600-ed s) and current oscillations specific for it, owing to unstable pittings which are re-passivated/activated. Similar behavior is also observed for the current transients of the  $Al_{(NaOH\&HNO_3)}/PhL_{(Na_3PO_4)}$  and  $Al_{(NaOH\&HNO_3)}/PhL_{(NH_4H_2PO_4)}$  systems (Fig. 8b, red 2 and green 3 curves, respectively).

The course of the current transients is again quite different for samples protected with CCOC and post-treated in phosphate solutions (Fig. 6b, blue 4, dark yellow 5 and magenta 6 curves, respectively). There are no current fluctuations characteristic for localized breakdown of the passive film, which leads to the initiation and growth of corrosion pits in CM. The transients have a course characteristic of processes of general corrosion.  $i_a$  of the  $Al_{(NaOH\&HNO_3)}/CCOC_{(Ce+Cu)}$  system increases gradually, coinciding with the transient for Al substrate ( $Al_{(NaOH\&HNO_3)}$ ) after about 1000-nd second. The chronoamperometric current transients characterizing the systems  $Al_{(NaOH\&HNO_3)}/CCOC_{(Ce+Cu)}/PhL_{(Na_3PO_4)}$  and  $Al_{(NaOH\&HNO_3)}/CCOC_{(Ce+Cu)}/PhL_{(NH_4H_2PO_4)}$  (Fig. 6b, dark yellow 5 and magenta 6 curves, respectively) remain lower. This difference in  $i_a$  drop is enhanced to  $2.6 \times 10^{-3}$

A.cm<sup>-2</sup> and  $1.7 \times 10^{-3}$  A.cm<sup>-2</sup>, respectively vs.  $3.4 \times 10^{-3}$  A.cm<sup>-2</sup> –  $i_a$  for the Al substrate.

*Investigations of Rp at E<sub>OCP</sub>. Comparison with the XPS data for the studied systems.* Fig. 7 shows histograms reflecting the changes in Rp of the studied systems as a function of exposure time (0.25 – 168/336 hours) in CM. Histograms 1–3 characterize the change in Rp for:  $Al_{(NaOH)}$  before (1) and after immersion treatment in Na<sub>3</sub>PO<sub>4</sub> (2) or NH<sub>4</sub>H<sub>2</sub>PO<sub>4</sub> (3); respectively for  $Al_{(NaOH\&HNO_3)}$  before (7) and after immersion treatment in Na<sub>3</sub>PO<sub>4</sub> (8) or NH<sub>4</sub>H<sub>2</sub>PO<sub>4</sub> (9). They indicate that the direct phosphate treatment of the Al substrate leads to a considerable increase in Rp (especially for the substrates  $Al_{(NaOH)}$ ), but that diminishes substantially upon reaching 168 h of exposure in CM. Histograms 4 – 6 in Fig. 7 characterize the change in Rp for the system  $Al_{(NaOH)}/CCOC_{(Ce+Cu)}$  before (4) and after immersion treatment in Na<sub>3</sub>PO<sub>4</sub> (5) or NH<sub>4</sub>H<sub>2</sub>PO<sub>4</sub> (6); respectively for  $Al_{(NaOH\&HNO_3)}/CCOC_{(Ce+Cu)}$  before (10) and after immersion treatment in Na<sub>3</sub>PO<sub>4</sub> (11) or NH<sub>4</sub>H<sub>2</sub>PO<sub>4</sub> (12). They show that the system  $Al_{(NaOH)}/CCOC_{(Ce+Cu)}$  and especially  $Al_{(NaOH\&HNO_3)}/CCOC_{(Ce+Cu)}$  are characterized by low Rp values. Its additional phosphate treatment in Na<sub>3</sub>PO<sub>4</sub> (5) and respectively (11) does not considerably increase Rp.

After post-treatment in NH<sub>4</sub>H<sub>2</sub>PO<sub>4</sub>, however, the change in Rp for the system  $Al_{(NaOH)}/CCOC_{(Ce+Cu)}/PhL_{(NH_4H_2PO_4)}$  over exposure time in CM increases systematically (up to ~ 1000 kΩ.cm<sup>2</sup>), oscillating during the interval of 144 – 288 h of exposure in CM. It begins to decline after 312 hours, reaching the even greater Rp value of ~ 160 kΩ.cm<sup>2</sup> at 336 hours. In the same time the value of Rp for the system  $Al_{(NaOH\&HNO_3)}/CCOC_{(Ce+Cu)}/PhL_{(NH_4H_2PO_4)}$  after the 168-th hour is lower than 30 kΩ.cm<sup>2</sup>.

The information obtained from the Rp method differs from that gathered *via* the “destructive” potentiodynamic polarization (PDP) curve method showed in Figs. 4 (a, b) and Table 3. Specifically, during measurements of Rp, the studied samples are under the influence of an  $E_{OCP}$ , except for a short period of time (~ 3 min), during which they are polarized and their Rp is measured. The Rp method lends the opportunity to assess the change in corrosion protective behavior of the studied systems during an actual corrosion process under conditions of self-dissolution (at  $E_{OCP}$ ), over a sufficiently long period of time. This assessment is usually associated with (change in) physical-chemical properties and composition of the conversion layers, as well as the influence of the formed corrosion products during extended exposure in the model corrosion medium. (The results obtained with this method are highly relevant to experiments/tests conducted in natural

corrosion conditions). In this aspect we have a reason to compare the  $R_p$  results obtained with the data detected by XPS analysis for the studied samples (Tables 4 and 5). The comparison and analysis of the obtained results give us a ground to conclude that:

- The type of pre-treatment of the Al substrate (in NaOH or in NaOH&HNO<sub>3</sub>) influences the content of Al(OH)<sub>3</sub>, non-stoichiometric AlOOH and Al<sub>2</sub>O<sub>3</sub> on its surface before and after deposition of CCOC and PhLs;

- The type of pre-treatment of the Al substrate strongly influences the content of ceria in as-deposited CCOC, their thickness respectively. Especially, the inclusion of an additional de-oxidation pre-treatment in HNO<sub>3</sub> increases the number of active sections (zones of island like Al<sub>3</sub>Fe phase as a rule coated by Cu) on the Al-1050 surface. In the same time these active sections (leading to the formation of galvanic pairs) can play negative role, provoking corrosion processes, increasing of  $i_{corr}$ ;

- The type of pre-treatment of the Al substrate influences strongly the time of exposure in CM at which the values of  $R_p$  are hold back enough high;

- The type of the phosphate post-treatment of the Al/CCOC/PhLs systems strongly influences the content of ceria in as-deposited CCOC, their thickness and composition, respectively. It is expressed in a strong decrease in the concentration of Al<sub>2</sub>O<sub>3</sub> and Ce<sub>2</sub>O<sub>3</sub>+CeO<sub>2</sub> components in CCOC at the expense of the formation of AlPO<sub>4</sub> and AlOOH, CePO<sub>4</sub> as well as PO<sub>3</sub><sup>-</sup>, P<sub>2</sub>O<sub>5</sub> and P<sub>4</sub>O<sub>10</sub> compounds with Al and Ce;

- Depending on the type of phosphate operation/solution (Na<sub>3</sub>PO<sub>4</sub> or NH<sub>4</sub>H<sub>2</sub>PO<sub>4</sub>), the CCOC can change the relation of Ce<sup>3+</sup> and Ce<sup>4+</sup> in the deep of mixed conversion layers, increasing the concentration of soluble Ce<sub>2</sub>O<sub>3</sub> and decreasing the low-soluble CeO<sub>2</sub>, respectively;

- The type of phosphate operation/solution strongly influences on the change/decrease of the  $R_p$  of the mixed CCOC and PhLs on the Al surface vs. time of exposure in the model corrosion medium.

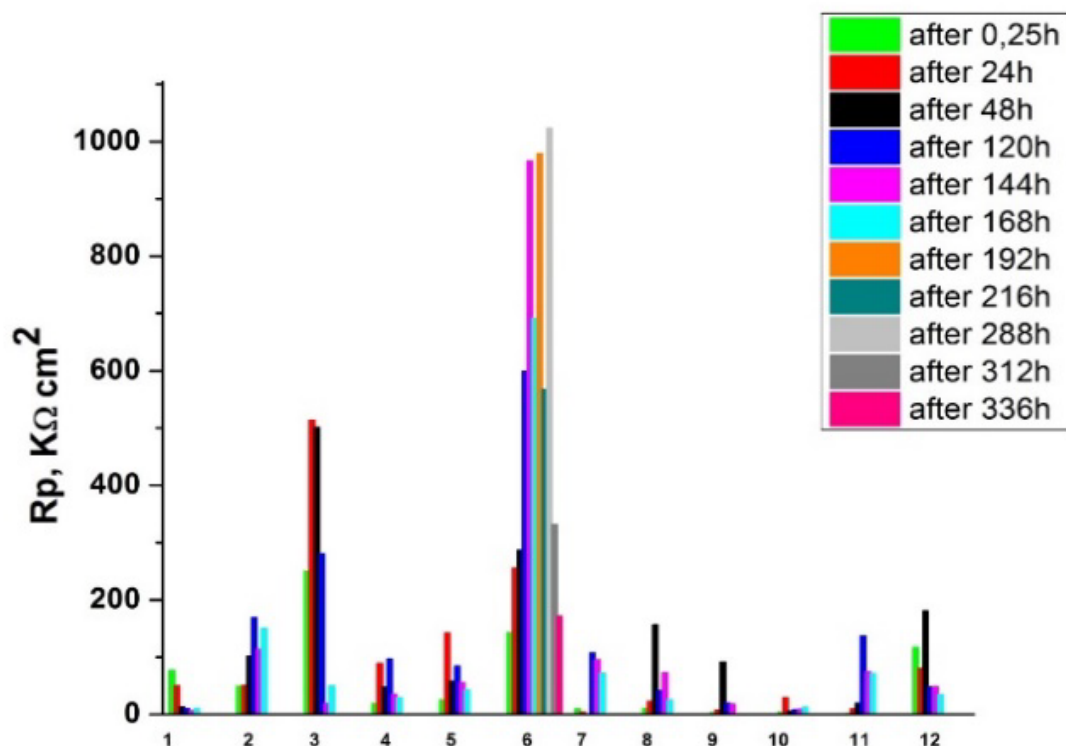


**Fig. 7.** Change in  $R_p$  (during exposure in 0.1 M NaCl.) of samples of Al 1050: pre-treated in 1.5 M NaOH (1); pre-treated in 1.5 M NaOH and post-treated by immersion in Na<sub>3</sub>PO<sub>4</sub> (2) or NH<sub>4</sub>H<sub>2</sub>PO<sub>4</sub> (3); pre-treated in 1.5 M NaOH and coated with CCOC (4); pre-treated in 1.5 M NaOH, coated with CCOC and post-treated in Na<sub>3</sub>PO<sub>4</sub> (5) or NH<sub>4</sub>H<sub>2</sub>PO<sub>4</sub> (6); or consecutively pre-treated in NaOH & HNO<sub>3</sub> (7); pre-treated in NaOH & HNO<sub>3</sub> and post-treated by immersion in Na<sub>3</sub>PO<sub>4</sub> (8); or NH<sub>4</sub>H<sub>2</sub>PO<sub>4</sub> (9); pre-treated in NaOH & HNO<sub>3</sub> and coated with CCOC (10); pre-treated in NaOH & HNO<sub>3</sub>, coated with CCOC and post-treated in Na<sub>3</sub>PO<sub>4</sub> (11) or NH<sub>4</sub>H<sub>2</sub>PO<sub>4</sub> (12).

**Table 4.** The quantitative electrochemical (Rp in kΩ cm<sup>2</sup> and CR in μm/year) and XPS (in at. %) results of: Al 1050 samples, pre-treated in NaOH (1) and post-treated in: Na<sub>3</sub>PO<sub>4</sub> (2); NH<sub>4</sub>H<sub>2</sub>PO<sub>4</sub> (3); coated with CCOC (4); coated with CCOC and post-treated in Na<sub>3</sub>PO<sub>4</sub> (5); coated with CCOC and post-treated in NH<sub>4</sub>H<sub>2</sub>PO<sub>4</sub> (6) - as deposited and after exposure in CM for 168 (and 336 for No 6) hours.

Sample	Rp, kΩ cm <sup>2</sup>	CR, μm/y	Chemical composition on the surface of the studied samples according to XPS investigations, at. %									
			O	Al	Ce (total) (Ce <sup>3+</sup> +Ce <sup>4+</sup> )	Cu	P	Fe	Cl	No	Ce <sup>4+</sup> , % of Ce (total)	
Al <sub>(NaOH)</sub> as pretreated	76.7	3.7	61.0	39.0	-	-	-	-	-	-	-	-
after 168 h in 0.1M NaCl	10.2	27.8	75.2	24.6	-	-	-	-	0.2	-	-	-
Al <sub>(NaOH)/PhL(Na<sub>3</sub>PO<sub>4</sub>)</sub> as deposited	49.0	5.7	58.4	28.2	-	-	12.1	1.3	0	-	-	-
after 168 h in 0.1M NaCl	150.4	1.9	76.3	22.0	-	-	1.4	-	0.3	-	-	-
Al <sub>(NaOH)/PhL(NH<sub>4</sub>H<sub>2</sub>PO<sub>4</sub>)</sub> as deposited	250	1.0	62.2	12.8	-	-	18.4	1.6	0	5	-	-
after 168 h in 0.1M NaCl	49.6	5.6	72.9	16.7	-	-	5.8	1.9	0.3	2.4	-	-
Al <sub>(NaOH)/CCOC(Ce+Cu)</sub> as deposited	18.9	11.8	71.9	21.2	6.9	-	-	-	0	-	-	79
after 168 h in 0.1M NaCl	29.7	9.6	74.8	22.1	1.5	1.1	-	-	0.5	-	-	37
Al <sub>(NaOH)/CCOC(Ce+Cu)/PhL(Na<sub>3</sub>PO<sub>4</sub>)</sub> as deposited	25.5	11.3	73.7	10.7	2.8	0	12.9	-	-	-	-	23
after 168 h in 0.1M NaCl	43.1	6.6	74.4	23.7	1.2	0.7	-	-	-	-	-	78
Al <sub>(NaOH)/CCOC(Ce+Cu)/PhL(NH<sub>4</sub>H<sub>2</sub>PO<sub>4</sub>)</sub> as deposited	143.2	2.0	76.3	7.6	1.4	0.6	14.1	-	-	-	-	11
after 168 h in 0.1M NaCl	691.8	0.4	72.4	19.1	0.8	0	7.7	0	0	0	0	0
after 336 h in 0.1M NaCl	171.7	2.0	74.3	7.8	5.4	0	5.2	0	0	7.3	17	-

**Table 5.** The quantitative electrochemical (Rp in kΩ cm<sup>2</sup> and CR in μm/year) and XPS (in at. %) results of: Al 1050 samples, pre-treated in NaOH&HNO<sub>3</sub> (1) and post-treated in: Na<sub>3</sub>PO<sub>4</sub> (2); NH<sub>4</sub>H<sub>2</sub>PO<sub>4</sub> (3); coated with CCOC (4); coated with CCOC and post-treated in Na<sub>3</sub>PO<sub>4</sub> (5); coated with CCOC and post-treated in NH<sub>4</sub>H<sub>2</sub>PO<sub>4</sub> (6) - as deposited and after exposure in CM for 168 hours.

Sample	Rp, KΩcm <sup>2</sup>	CR, μm/y	Chemical composition on the surface of the studied samples according to XPS investigations, at. %										
			O	Al	Ce (total) (Ce <sup>3+</sup> +Ce <sup>4+</sup> )	Cu	P	Fe	Cl	N	Na	Ce <sup>4+</sup> , % of Ce (total)	
Al <sub>(NaOH&amp;HNO<sub>3</sub>)</sub> as pretreated	9.5	30.0	59.1	40.9									
after 168h in 0.1M NaCl	71.8	4.0	81.1	18.0				0.4	0.5				
Al <sub>(NaOH&amp;HNO<sub>3</sub>)</sub> /PhL <sub>(Na<sub>3</sub>PO<sub>4</sub>)</sub> as deposited	10.4	27.2	68.9	23.0			2.9	5.2					
after 168h in 0.1M NaCl	25.3	11.2	79.8	17.4			0.1	0.7			2.0		
Al <sub>(NaOH&amp;HNO<sub>3</sub>)</sub> /PhL <sub>(NH<sub>4</sub>H<sub>2</sub>PO<sub>4</sub>)</sub> as deposited	3.1	93.2	63.7	24.0			10.6	0.6		1.1			
after 168h in 0.1M NaCl	14.8	19.1	70.9	22.1					2.7		4.3		
Al <sub>(NaOH&amp;HNO<sub>3</sub>)</sub> /CCOC <sub>(Ce+Cu)</sub> as deposited	4.1	69.0	76.5		13.8		4.5		5.2				100
after 168h in 0.1M NaCl	12.2	23.3	73	23.5			2.5		0.2	0.8			
Al <sub>(NaOH&amp;HNO<sub>3</sub>)</sub> /CCOC <sub>(Ce+Cu)</sub> / PhL <sub>(Na<sub>3</sub>PO<sub>4</sub>)</sub> as deposited	1.5	187.5	70.1	23.8				3.5	2.6				
after 168h in 0.1M NaCl	71.0	4.0	83.8	15.6			0.3			0.3			
Al <sub>(NaOH&amp;HNO<sub>3</sub>)</sub> /CCOC <sub>(Ce+Cu)</sub> / PhL <sub>(NH<sub>4</sub>H<sub>2</sub>PO<sub>4</sub>)</sub> as deposited	117.0	2.4	67.9	14.4	0.8			13.2	0.6		2.2	0.9	8
after 168h in 0.1M NaCl	34.6	8.2	75.2	18.0	0.2			3.0	0.5		2.4	0.7	0

Consideration of Rp at E<sub>OCP</sub> and CR of the studied systems. On Fig. 8 are shown the results obtained for the systems of Al substrates which are pre-treated in NaOH (Fig. 8a) or consecutively in NaOH and HNO<sub>3</sub> (Fig. 8b). Fig. 8a, in which exposure time in CM is plotted on the X-axis, simultaneously illustrates the course of change in Rp (left ordinate) and CR (right ordinate) for the investigated systems. Our results indicate that the most effective, from a corrosion perspective, is the protection of Al 1050, based on the consecutive pre-treatment in NaOH and formation of conversion layers of CCOC and PhL, deposited in NH<sub>4</sub>H<sub>2</sub>PO<sub>4</sub>. In this case, the values of CR are of the order of 0.8 μm/y, while with post-treatment with Na<sub>3</sub>PO<sub>4</sub> the range is 5.5 μm/y (the value for the unprotected Al substrate - 25 μm/y).

The analysis of these results and their comparison to the data for the changes in the concentrations of Ce<sup>3+</sup>/Ce<sup>4+</sup> and P (resp. Ce<sub>2</sub>O<sub>3</sub>, CeO<sub>2</sub>, AlPO<sub>4</sub> and AlOOH, CePO<sub>4</sub> as well as PO<sub>3</sub><sup>-</sup>, P<sub>2</sub>O<sub>5</sub> and P<sub>4</sub>O<sub>10</sub> compounds with Al and Ce) on the surface of the formed conversion layers (during the time of

exposure in CM - Tables 4, 5 and 2) indicates a direct correlation between these two aspects. Also, the formation of AlPO<sub>4</sub> and CePO<sub>4</sub> leads to considerable increase in Rp of the mixed CCOC/PhL conversion coating. At the same time increased duration of exposure in CM leads to a decrease in the concentrations of Al<sub>2</sub>O<sub>3</sub> and Ce<sub>2</sub>O<sub>3</sub>+CeO<sub>2</sub> (as components in CCOC) at the expense of the formation of AlPO<sub>4</sub> and AlOOH, CePO<sub>4</sub>, as well as PO<sub>3</sub><sup>-</sup>, P<sub>2</sub>O<sub>5</sub> and P<sub>4</sub>O<sub>10</sub> compounds of Al and Ce in the mixed conversion layers. As a result of this higher Rp values which determine lower values of CR (Fig. 8a) are achieved and maintained. In this aspect the maximum effect is reached for the system Al<sub>(NaOH)</sub>/CCOC<sub>(Ce+Cu)</sub>/PhL<sub>(NH<sub>4</sub>H<sub>2</sub>PO<sub>4</sub>)</sub>.

On Fig. 8b are shown the results reflecting the changes in Rp and CR of the studied systems, the Al substrates of which are pre-treated in NaOH and HNO<sub>3</sub>. The analysis of the results obtained showed that at the direct immersion treatment of the Al substrate (Al<sub>(NaOH&HNO<sub>3</sub>)</sub>) by PhLs better results from a corrosion point of view determine the post-treatment by Na<sub>3</sub>PO<sub>4</sub>. However, highly impressive is

the effect of this phosphate post-treatment for the Rp and CR at the time of exposure only till 48-th h.

CCOC, deposited on  $Al_{(NaOH\&HNO_3)}$  (the  $Al_{(NaOH\&HNO_3)}/CCOC_{(Ce+Cu)}$  system), is characterized by lowest indices in comparison to these for the systems  $Al_{(NaOH\&HNO_3)}/PhLs$ , more probably because of the higher concentration of Cu and Fe ( $Al_3Fe$ ) sections in them (Table 5) [17]. The phosphate(s) processing of the  $Al_{(NaOH\&HNO_3)}/CCOC_{(Ce+Cu)}$  system however improves substantially the protective indicators of the mixed  $Al_{(NaOH\&HNO_3)}/CCOC_{(Ce+Cu)}/PhLs$  systems. This improvement is connected with a noteworthy decrease of the deviations of Rp and  $i_a$  (Fig. 8b) starting from the beginning of exposure in CM. At this reached maximum protective effect is for the system  $Al_{(NaOH\&HNO_3)}/CCOC_{(Ce+Cu)}/PhL_{(NH_4H_2PO_4)}$ . The deviations and oscillations in Rp and CR (corresponding  $E_{cor}$  and  $i_a$ ), respectively, for this system are decreased and stabilized in maximum degree.

### CONCLUSION

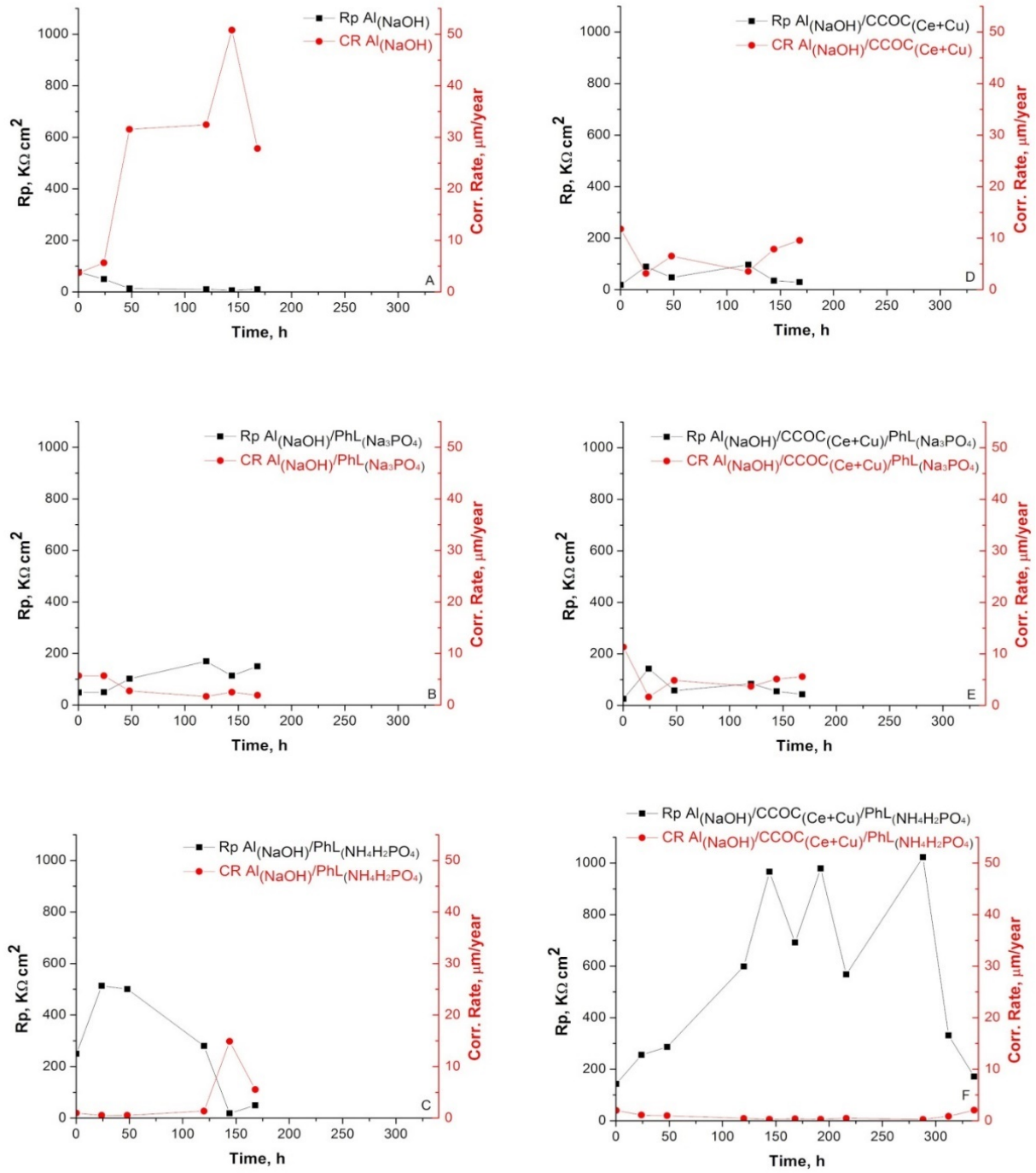
Ceria-based conversion coatings, formed on technically pure Al-1050, were post-treated in phosphate containing solutions. We paid extra attention to the influence of the type of “pre-” and “post-treatment” operations.

The chemical composition on the surface of the obtained conversion systems was characterized by means of X-ray photoelectron spectroscopy. Based on the obtained results it was ascertained that there is substantial influence of the “pre-treatment” and “post-treatment” operations on the chemical composition and chemical state of the elements on their surface. It is expressed by a strong decrease in the concentration of  $Al_2O_3$  and  $Ce_2O_3+CeO_2$  components in the as-deposited CCOCs at the

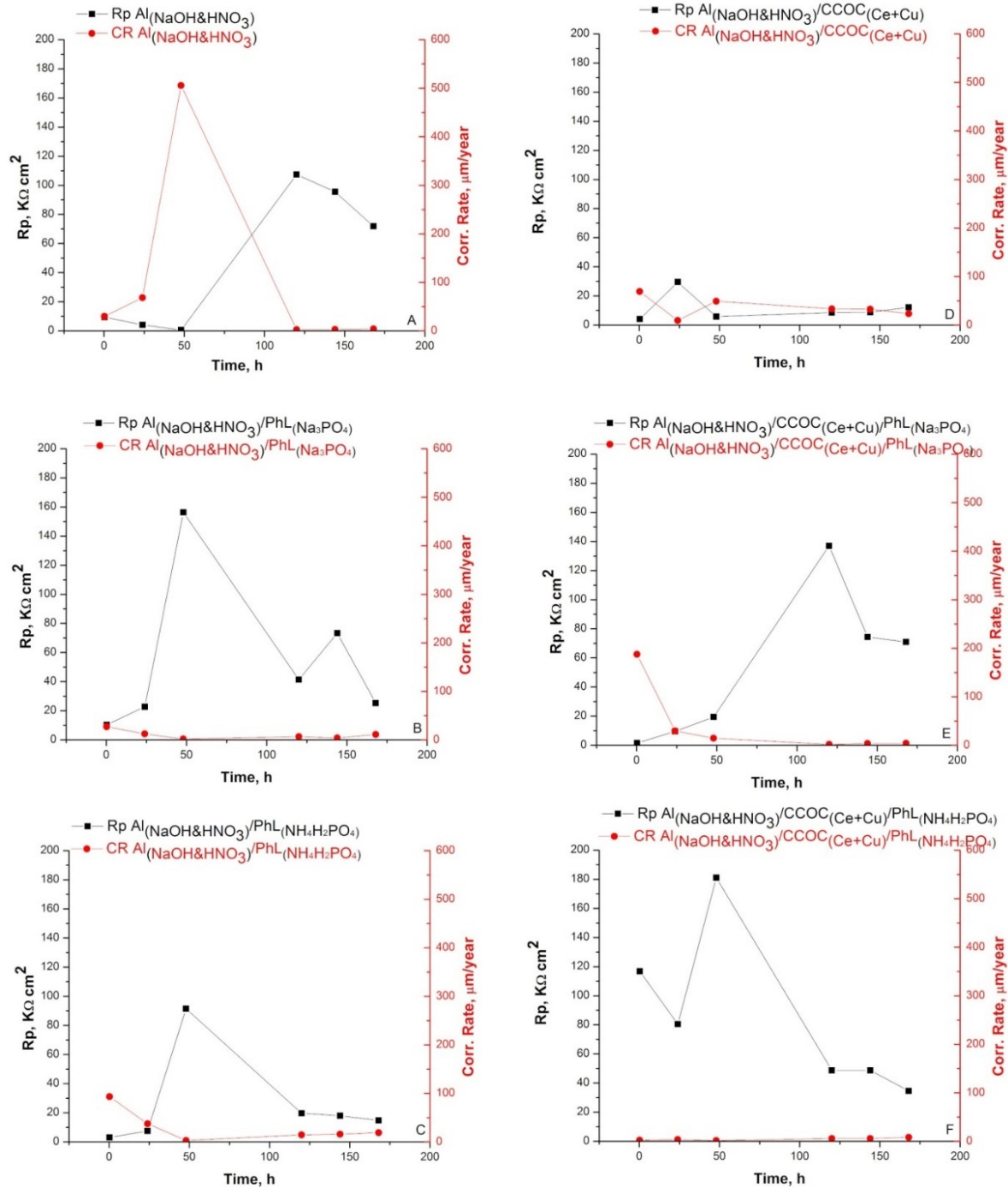
expense of formation of  $AlPO_4$  and  $AlOOH$ ,  $CePO_4$  as well as  $PO_3^-$ ,  $P_2O_5$  and  $P_4O_{10}$  compounds with Al and Ce, after their post-treatment in phosphate solutions.

Electrochemical and corrosion investigations and the determination of the basic corrosion parameters as  $E_{cor}$ ,  $i_{cor}$ ,  $Z$ ,  $E_{OCP}$ ,  $i_a$ ,  $E_{pit}$ , Rp and CR of the studied systems (as-deposited and after definite time of exposure in a model 0.1M NaCl corrosion medium) were carried out. The comparison of these results with the changes in the concentrations of  $Ce^{3+}/Ce^{4+}$ , Al and P (their respective oxides and phosphates) before and after exposure of the samples in CM shows that the concentrations of  $Ce^{4+}$  and P on the surface of the studied samples are directly related. Polarization investigations simultaneously showed that the combined phosphate and ceria conversion layers are not only static barrier coatings, but they also change the kinetics of the conjugated electrochemical reactions characterizing the corrosion process in  $Cl^-$  containing media, i.e. they determine the electrochemical protection of Al substrate.

The established protective effect of the mixed conversion coatings on Al at long exposure in CM can be related to the beneficial transformation of the chemical composition of CCOC, formed on Al substrates after phosphate processing. This effect, as well as the formation of different types of corrosion products on the surface of  $Al/CCOC/PhLs$  systems, provide an effective barrier to the diffusion of  $Cl^-$  to the Al surface, which leads to corresponding positive and beneficial changes of the Rp and CR for the studied systems.



(a)



(b)

**Fig. 8.** Change in Rp and CR of the studied systems: Al substrate(s) of which are pretreated in 1.5 M NaOH (a) or in 1.5 M NaOH& 5M HNO<sub>3</sub> (b) during exposure in 0.1M NaCl.

**Acknowledgement:** The authors are grateful to acknowledge: „Equipment supported/obtained under the project INFRAMAT (National Roadmap for Research Infrastructure) financed by Bulgarian Ministry of Education and Science was used in this investigation“; support from the CoC „Clean technologies for sustainable environment – water, waste, energy for circular economy“, (Project BG05M2OP001-1.002-0019), supported by the ERDF within the Bulgarian OP “SESG 2014–2020“ and the support from the CoE

“National center for/of mechatronics and clean technologies” (Project BG05M2OP001–1.001–0008) supported by the ERDF within the Bulgarian OP “SESG 2014–2020.“

#### REFERENCES

1. B. Hinton, *Corrosion*, **66**, 1 (2010).
2. S. Wernick, R. Pinner, P. Sheasby, ‘The Surface Treatments of Aluminium and Its Alloys’, 5th edn., ASM International and Finishing Publications Ltd.,

- M Metals Park, Ohio, 1987.
3. Official Journal of the European Union, 'COMMISSION DIRECTIVE (EU) 2017/ 2096 - of 15 November 2017 - Amending Annex II to Directive 2000/ 53/ EC of the European Parliament and of the Council on End-of Life Vehicles'(2017).
  4. Official Journal of the European Union, 'COMMISSION IMPLEMENTING DECISION (EU) 2019/2193 of 17 December 2019 Laying down Rules for the Calculation, Verification and Reporting of Data and Establishing Data Formats for the Purposes of Directive 2012/19/EU of the European Parliament and of the Council on Waste Electrical and Electronic Equipment (WEEE)' (2019).
  5. T. G. Harvey, *Corros. Eng. Sci. Technol.*, **48**, 248 (2013).
  6. C. Girginov, S. Kozhukharov, in: Extended Abstracts of 7<sup>th</sup> Regional RSE-SEE Symposium on Electrochemistry and 8<sup>th</sup> Kurt Schwabe Symposium, V. Horvat-Radošević, K. Kvastek, Z. Mandić (eds.), International Association of Physical Chemists, Split, Croatia, 132 (2019).
  7. C. E. Castano, W. G. Fahrenholtz, M. J. O'Keefe, in: Metal oxides, Elsevier's Book series "Ceria-Based Coatings and Pigments - Synthesis, Properties and Applications", 2020, p. 211.
  8. S. Kozhukharov, C. Girginov, in: NATO Science for Peace and Security Series B: Physics and Biophysics, P. Petkov, M. Achour, C. Popov (eds.), Springer, Dordrecht, 2020, p. 437.
  9. Q. Zhu, B. Zhang, X. Zhao, B. Wang, *Coatings*, **10**, 128 (2020).
  10. J. So, E. Choi, J. T. Kim, J. S. Shin, J. B. Song, M. Kim, C. W. Chung, J. Y. Yun, *Coatings*, **10**, 103 (2020).
  11. F. Czerwinski, *Journal of Materials Science*, **55**, 24 (2020).
  12. D. K. Heller, W. G. Fahrenholtz, M. J. O'Keefe, *Corros. Sci.*, **52**, 360 (2010).
  13. R. Andreeva, E. Stoyanova, A. Tsanev, D. Stoychev, *Comptes Rendus de l'Académie Bulg. des Sci.*, **72**, 1336 (2019).
  14. R. Andreeva, E. Stoyanova, A. Tsanev, D. Stoychev, *J. Phys. Conf. Ser.*, **700**(1), 012049 (2016).
  15. R. Andreeva, E. Stoyanova, A. Tsanev, P. Stefanov, D. Stoychev, *Trans. IMF*, **92**, 203 (2014).
  16. R. Andreeva, E. Stoyanova, D. Stoychev, *J. Int. Sci. Publ. Mater. Methods Technol.*, **8**, 751 (2014).
  17. E. Stoyanova, D. Stoychev, *J. Appl. Electrochem.*, **27**, 685 (1997).
  18. R. Andreeva, E. Stoyanova, A. Tsanev, M. Datcheva, D. Stoychev, *Int. J. Electrochem. Sci.*, **13**, 5333 (2018).
  19. H. Zhang, Y. Zuo, *Appl. Surf. Sci.*, **254**, 4930 (2008).
  20. H. Hasannejad, M. Aliofkhaezrai, A. Shanaghi, T. Shahrabi, A. R. Sabour, *Thin Solid Films*, **517**, 4792 (2009).
  21. W. Pinc, P. Yu, M. O'Keefe, W. Fahrenholtz, *Surf. Coatings Technol.*, **203**, 3533 (2009).
  22. D. K. Heller, W. G. Fahrenholtz, M. J. O'Keefe, *J. Electrochem. Soc.*, **156**, 400 (2009).
  23. R. Andreeva, E. Stoyanova, A. Tsanev, D. Stoychev, *J. Phys. Conf. Ser.* **1492**(1), 012019 (2020).
  24. S. Damyanova, C. A. Perez, M. Schmal, J.M.C. Bueno, *Appl. Catal. A Gen.*, **234**, 271 (2002).
  25. E. Bêche, P. Charvin, D. Perarnau, S. Abanades, G. Flamant, *Surf. Interface Anal.*, **40**, 264 (2008).
  26. X. Yu, G. Li, *J. Alloys Compd.*, **364**, 193 (2004).
  27. C. Girginov, I. Avramova, S. Kozhukharov, *J. Chem. Technol. Metall.*, **51**, 705 (2016).
  28. R. Kumar, J. Rashid, M. A. Barakat, *RSC Adv.*, **4**, 38334 (2014).
  29. M. Shimizu, Y. Tsushima, S. Arai, *ACS Omega*, **2**, 4306 (2017).
  30. S. Bernal, G. A. Cifredo, J. M. Rodríguez-Izquierdo, *Artic. J. Phys. Chem. C*, **99**, 11794 (1995).
  31. S. Fan, C. Yang, L. He, J. Deng, L. Zhang, L. Cheng, *Tribol. Int.*, **114**, 337 (2017).
  32. I. Danilidis, J. Hunter, G. M. Scamans, J. M. Sykes, *Corros. Sci.*, **49**, 1559 (2007).
  33. H. Zhang, G. Yao, S. Wang, Y. Liu, H. Luo, *Surf. Coatings Technol.*, **202** 1825 (2008).
  34. Z. Szklarska-Smialowska, *Corros. Sci.*, **41**, 1743 (1999).